Controlling the spectral response in guided-mode resonance filter design

Samuel T. Thurman and G. Michael Morris

Techniques for controlling spectral width are used in conjunction with thin-film techniques in the design of guided-mode resonance (GMR) filters to provide simultaneous control over line-shape symmetry, sideband levels, and spectral width. Several factors that could limit the minimum spectral width are discussed. We used interference effects for passband shaping by stacking multiple GMR filters on top of one another. A design is presented for a 200-GHz telecommunications filter along with a tolerance analysis. Compared with a conventional thin-film filter, the GMR filter has fewer layers and looser thickness tolerances. Grating fabrication tolerances are also discussed.

OCIS codes: 050.2770, 120.2440, 260.5740, 240.0310.

1. Introduction

Perhaps the most common type of optical filter is the thin-film filter.[1] Thin-film filters are used widely as narrowband filters in laser cavities, light modulators, and optical telecommunication components. Some advantages of thin-film optics are high efficiency and versatility. However, narrowband filters with subnanometer passbands are difficult to fabricate. For example, thin-film filters for wavelength division multiplexing (WDM) applications often have more than a hundred individual layers with stringent tolerances on each layer.[2] Guided-mode resonance (GMR) filters are a new class of narrowband filters that could be important in a number of applications. Suggested applications include laser cavity reflectors,[3,4] polarizers,[3] light modulators,[5] biosensors,[6] and WDM filters.[7] One advantage of GMR filters is that they operate on a resonance effect, which can be exhibited by relatively simple structures. Thus, it might be possible to replace a many-layered thin-film filter with a GMR filter that has much fewer layers.

The resonance effect is associated with leaky modes that are supported by GMR structures. All the structures that we consider in this paper have a waveguide layer and a grating layer. In the absence of the grating, the waveguide would support a true bound mode. However, the mode becomes leaky when the grating layer is added, as energy is coupled out of the waveguide into radiation modes. Conversely, energy could be coupled from an incident plane wave into the waveguide. At resonance, energy from an incident plane wave is coupled into a leaky mode and then back into one or more radiation modes. The coupling is highly sensitive to the wavelength of light and angle of incidence, and a sharp resonant peak might be observed in the reflected light when either of these parameters is varied.

GMR filters have been studied for several years, yet their versatility has not been fully realized. To make GMR filters for practical applications, one needs to exercise control over the various features of a filter's spectral response, such as symmetry, sideband suppression, spectral width, and passband shape. Although researchers have investigated various factors affecting symmetry and sideband suppression[8,9] spectral width,[10–14] and passband shape,[15] analytic design methods for simultaneous control over all these features have not been developed. Tibuleac and Magnusson[16] presented designs based on a numerical routine that demonstrated control over symmetry, sideband levels, and passband width. This paper presents analytic design methods for controlling all four of these line-shape features simultaneously. In Section 2 we discuss control over symmetry and sideband suppression based on an improved version of the thin-film design method.[8,17] In Section 3 we

S. T. Thurman (thurman@optics.rochester.edu) is with The Institute of Optics, University of Rochester, Rochester, New York 14627. G. M. Morris is with Corning Rochester Photonics Corporation, Rochester, New York 14626.

Received 21 February 2003.
0003-6935/03/163225-09$15.00/0

present examples that integrate techniques for controlling spectral width into the thin-film design method, demonstrating simultaneous control over symmetry, sideband suppression, and spectral width. Also, several factors that could limit the minimum spectral width are discussed. In Section 4 we present a technique for added control over the passband shape based on interference effects,[15] and a 200-GHz WDM filter is presented as an example. Section 5 discusses the fabrication tolerances for the 200-GHz filter and shows that the thickness tolerances for the GMR filter are much looser than those for a conventional thin-film design. Grating tolerances and efficiency requirements are discussed also. Rigorous coupled-wave analysis (RCWA)[18,19] is used to calculate the spectral response for all the GMR filters in this paper. A waveguide perturbation method[20] is used to investigate the relationship between specific design parameters and spectral width. All the examples in this paper are one-dimensional structures that operate with TE-polarized light (electric field perpendicular to the grating vector in a classical mounting). However, the principles that we present might be applied to structures that operate with TM-polarized light and two-dimensional structures, which could be made polarization independent.

2. Symmetry and Sideband Suppression

In 1994 Wang and Magnusson[8] showed that it is useful to look at a GMR filter as an effective thin-film stack. They used an effective medium theory (EMT) to model a grating layer as a homogeneous thin-film layer having some effective index of refraction. Then they chose various layer thicknesses for a filter based on traditional thin-film techniques in an effort to achieve a symmetric spectral response with low sidebands. We refer to this method of choosing the layer thicknesses as the thin-film design method. The principle for inducing symmetry and suppressing sidebands in the thin-film method is to design the effective thin-film stack to be antireflective at the resonant wavelength. In 2000, Hegedus and Netterfield[9] suggested that the thin-film method is inadequate for designing symmetric filters. They cited several filter examples based on the thin-film method that were not symmetric on a logarithmic scale. They suggested a numerically intensive design method based on rigorous modeling as an alternative. However, as we have shown,[17] the results of the thin-film method are dependent on the effective-index model used for the grating layer.

In 1956, Rytov[21] developed an EMT for finely stratified media and derived a transcendental equation relating the effective index to the physical parameters of a stratified medium and the wavelength of light. Rytov's theory can be applied to the grating

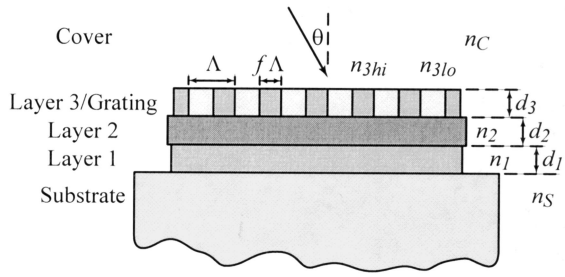

Fig. 1. Illustration of a three-layer GMR filter; n_s, n_1, n_2, and n_c are the indices of the substrate, layer 1, layer 2, and the cover region; d_1, d_2, and d_3 are the layer thicknesses; $n_{3\mathrm{hi}}$ and $n_{3\mathrm{lo}}$ represent the high and low indices of the grating layer; Λ is the grating period; f is the grating fill factor, and θ is the angle of incidence.

problem and written in the following form for TE-polarized light:

$$(n_{\mathrm{hi}}^2 - n_{\mathrm{eff}}^2)^{1/2} \tan[\pi(n_{\mathrm{hi}}^2 - n_{\mathrm{eff}}^2)^{1/2} f\Lambda/\lambda] = -(n_{\mathrm{lo}}^2 - n_{\mathrm{eff}}^2)^{1/2} \tan[\pi(n_{\mathrm{lo}}^2 - n_{\mathrm{eff}}^2)^{1/2} \times (1-f)\Lambda/\lambda], \quad (1)$$

where n_{hi} and n_{lo} are the high and low indices of refraction for the grating, n_{eff} is the effective index of refraction, f is the fill factor or duty cycle of the grating, Λ is the grating period, and λ is the wavelength of light. For a specified grating, this equation must be solved numerically to determine the effective index. In the limit of long wavelength ($\Lambda/\lambda \to 0$), Eq. (1) reduces to an analytic expression for the effective index:

$$n_{\mathrm{eff}} = [f n_{\mathrm{hi}}^2 + (1-f) n_{\mathrm{lo}}^2]^{1/2}. \quad (2)$$

Equation (1) will be referred to as the exact effective-index model, whereas Eq. (2) will be referred to as the zeroth-order effective-index model. In all the examples cited by Hegedus and Netterfield, the zeroth-order effective-index model was used with the thin-film method, even though the period-to-wavelength ratios were rather large ($\Lambda/\lambda \cong 0.6$). In such cases when a long-wavelength approximation is not well justified, it is more appropriate to use the exact effective-index model.[17]

Consider the design of a three-layer GMR filter based on the geometry shown in Fig. 1. In this example, layer 1 is a subwaveguide layer, layer 2 is a waveguide layer, and layer 3 is a grating. The grating layer couples light from an incident plane wave into a leaky mode that is localized to the waveguide layer. The purpose of the subwaveguide layer is to reduce the sidebands by improving the antireflective properties of the effective thin-film stack. Using the thin-film method, we chose the layer thicknesses to make the effective thin-film stack antireflective at the resonant wavelength. Figure 2 compares the spectral response for two filters based on the thin-film method. The dashed curve represents a filter based on the zeroth-order effective-index model. Note that errors in the effective index for the grating lead to asymmetry in the spectral response. This

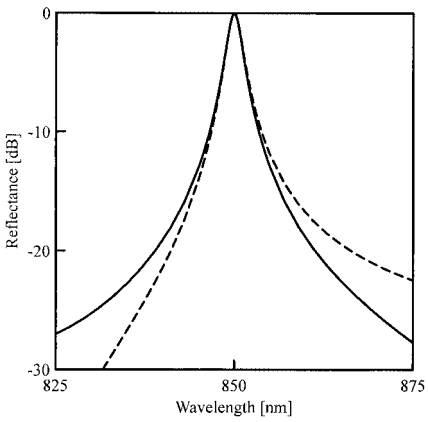

Fig. 2. Spectral response for two three-layer GMR filters. Both filters are based on the thin-film method: the dashed curve represents a filter taken from Fig. 3 of Ref. 4, which is based on the zeroth-order effective-index model with $f = 50\%$; the solid curve represents a filter based on the exact effective-index model with $f = 42\%$. The remaining design parameters are the same for both filters: $n_s = 1.453$, $n_1 = 2.005$, $n_2 = 2.106$, $n_{3\mathrm{hi}} = 1.490$, $n_{3\mathrm{lo}} = n_c = 1.000$, $d_1 = 106$ nm, $d_2 = 101$ nm, $d_3 = 168$ nm, $\Lambda = 483$ nm, and $\theta = 0$ deg.

design was cited by Hegedus and Netterfield as an example of when the thin-film method failed. The solid curve in Fig. 2 represents a design based on the exact effective-index model. The grating fill factor was adjusted for this filter until the effective index was equal to the index that was used to design the filter. Note that the results of the thin-film method might be improved by use of the appropriate effective-index model. It is noted that the EMT is approximate and as a result filters based on the thin-film method sometimes exhibit asymmetry, especially when the resonant peak is narrow. As we show in Section 3, such asymmetry might be removed by adjustment of the grating depth and/or fill factor. Also, it is noted that Lorentzian-like behavior near resonance sets a lower bound on the sideband levels.

3. Spectral Width

As mentioned in Section 1, the resonance effect is associated with a leaky mode supported by the GMR structure. The propagation coefficient of a leaky mode is complex and can be written as

$$\beta = \beta_0 + i\gamma\,, \tag{3}$$

where β_0 and γ are purely real and i is the imaginary number. The imaginary part of the propagation coefficient γ is interpreted as the loss of the leaky mode. It is generally understood that the spectral width of a resonant peak is proportional to this loss parameter.[10,22] Norton *et al.*[12] showed that, for a resonance associated with a single leaky mode, the full spectral width at half-maximum is approximately given by

$$\Delta\lambda_{\mathrm{FWHM}} = \lambda_0\Lambda\gamma/\pi\,, \tag{4}$$

where λ_0 is the resonant wavelength, Λ is the grating period, and γ is determined at the resonant wavelength. Therefore, to control spectral width, one must be able to control the loss of the leaky mode.

Many of the factors used to control the loss also affect other spectral features. For example, Fano[10] considered loss that is due to material absorption and predicted that an increase in absorption would lead to an increase in the spectral width. Although this is true, increasing the absorption comes at the price of decreased peak efficiency. Norton *et al.* showed how the grating depth[12] and grating modulation[13] contribute to coupling loss and affect the spectral width. However, these parameters also play key roles in the determination of spectral symmetry and sideband suppression. Here we are interested in combining techniques for controlling spectral width with the thin-film method, which is used for controlling symmetry and sideband levels. We accomplished this by designing the effective thin-film stack with some layer thickness that might be varied to control the coupling loss of the leaky mode while maintaining the antireflective properties of the stack. At first, it might seem difficult to design a filter that meets these requirements, but in practice it is actually quite simple.

Recently, Levy-Yurista and Friesem[14] showed that a buffer layer introduced between the grating and the waveguide layers could be used to control spectral width. We consider a structure similar to theirs but examine conditions for preserving symmetry and sideband suppression as the spectral width is adjusted. The three-layer filter geometry shown in Fig. 1 will be used. Now, layer 1 is the waveguide layer, and layer 2 is a buffer layer. The leaky mode is still localized in the waveguide layer, but the thickness of the buffer layer controls the coupling loss of the leaky mode. If the buffer layer thickness is increased, the grating is pushed farther away from the waveguide layer, lowering the coupling loss and producing a narrower spectral width. The conditions for preserving symmetry and sideband suppression can be met by designing the grating layer as a quarter-wave antireflection layer between the cover region and the buffer layer, making the waveguide layer half-wave, and matching the indices of the buffer and the substrate materials. Figure 3 shows the spectral response for such a series of GMR filters with various buffer layer thicknesses. The grating period was adjusted along with the buffer thickness to maintain the same resonant wavelength. Note that the width of the resonant peak decreases as the buffer layer thickness increases and that symmetry and sideband suppression are nearly preserved. As the spectral width becomes narrower, the spectral response is more sensitive to errors introduced by the EMT and the line shape becomes asymmetric. Figure 4 shows the relationship between the spectral width and the thickness of the buffer layer. Note that the spectral width is exponentially dependent on the buffer layer thickness.

The same principles for controlling the spectral response can be applied to other filter geometries. Figure 5 shows a five-layer GMR filter geometry. In

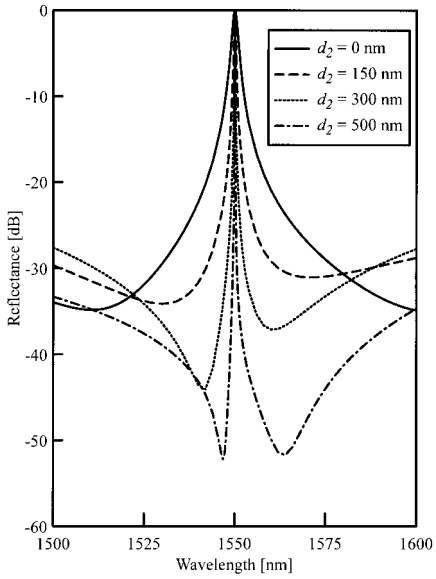

Fig. 3. Spectral response for a series of three-layer GMR filters with various buffer layer thicknesses. The solid curve represents a filter with $d_2 = 0$ nm and $\Lambda = 855$ nm; the dashed curve represents a filter with $d_2 = 150$ nm and $\Lambda = 846$ nm; the dotted curve represents a filter with $d_2 = 300$ nm and $\Lambda = 843$ nm; the dash–dot curve represents a filter with $d_2 = 500$ nm and $\Lambda = 842$ nm. The remaining design parameters are the same for each filter: $n_s = n_2 = n_{3hi} = 1.500$, $n_1 = 2.000$, $n_{3lo} = n_c = 1.000$, $d_1 = 388$ nm, $d_3 = 317$ nm, $f = 33\%$, and $\theta = 5$ deg.

this example layers 1 and 2 are designed to be antireflective between the substrate and layer 3, which is a waveguiding layer. This is done by choosing the thickness of layers 1 and 2 based on a traditional V-coat design.[1] Instead of a quarter-wave grating layer on top of the filter, layers 4 and 5 together are designed to be antireflective between the cover region and the waveguide layer in a manner analogous to a V coat. Here, the thickness of the waveguide layer is

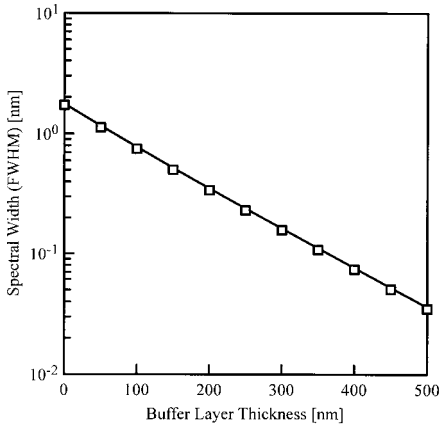

Fig. 4. Relationship between spectral width and buffer layer thickness for the series of GMR filters in Fig. 3. The squares represent data from RCWA calculations and the line represents calculations based on Eq. (4), where a waveguide perturbation method[20] is used to estimate the loss of leaky mode γ. The design parameters are the same as for the filters in Fig. 3.

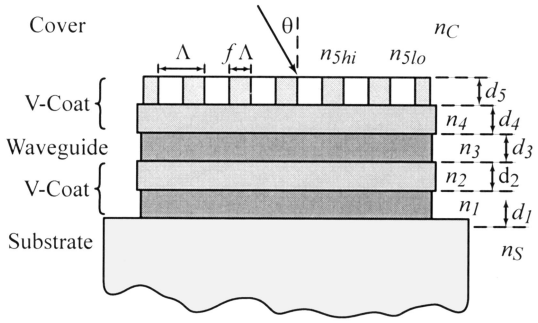

Fig. 5. Illustration of a five-layer GMR filter made up of a V coat, a waveguide layer, and another V coat that includes a grating layer.

used to control spectral width. When the waveguide thickness increases, the leaky mode associated with the resonance becomes more localized in the waveguide layer, decreasing the coupling loss and producing a narrower spectral width. We controlled symmetry and sideband suppression by designing layers 4 and 5 as a V coat between the cover region and the waveguide material and layers 1 and 2 as a V coat between the waveguide material and the substrate. Figure 6 shows the spectral response for a series of such GMR filters with various waveguide thicknesses. For these filters we used the thin-film method to determine the grating layer thickness, assuming the effective index of the grating was 1.250.

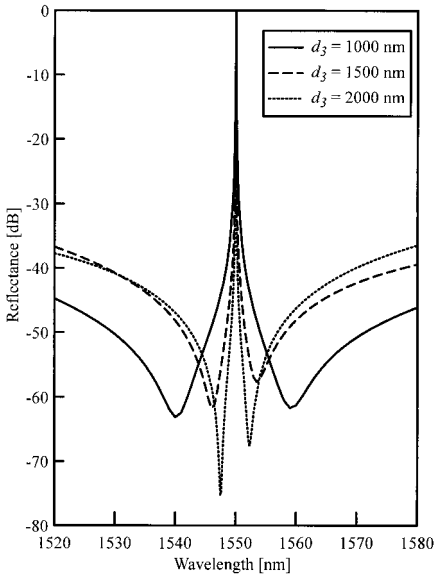

Fig. 6. Spectral response for a series of five-layer GMR filters based on the geometry of Fig. 5 with various waveguide layer thicknesses. The solid curve represents a filter with $d_3 = 1000$ nm, $\Lambda = 739$ nm, and $f = 41.2\%$; the dashed curve represents a filter with $d_3 = 1500$ nm, $\Lambda = 727$ nm, and $f = 41.3\%$; the dotted curve represents a filter with $d_3 = 2000$ nm, $\Lambda = 722$ nm, and $f = 41.4\%$. The remaining design parameters are the same for each filter: $n_s = n_2 = n_4 = n_{5hi} = 1.500$, $n_1 = n_3 = 2.000$, $n_{5lo} = n_c = 1.000$, $d_1 = 64$ nm, $d_2 = 86$ nm, $d_4 = 186$ nm, $d_5 = 160$ nm, and $\theta = 10$ deg.

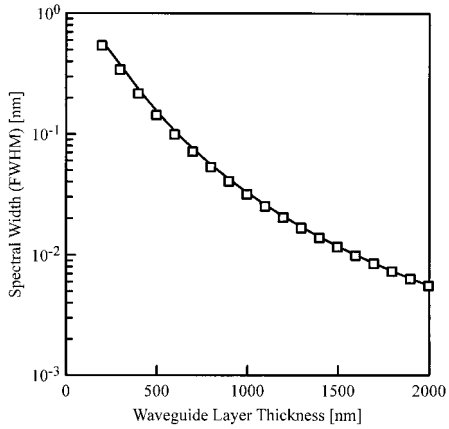

Fig. 7. Relationship between spectral width and waveguide layer thickness for the series of GMR filters in Fig. 6. The squares represent data from RCWA calculations and the curve represents calculations based on Eq. (4), where a waveguide perturbation method[20] is used to estimate the loss of leaky mode γ. The design parameters are the same as for the filters in Fig. 6.

As the waveguide layer thickness was increased, the grating period was adjusted to maintain the same resonant wavelength, and the grating fill factor was adjusted to optimize the performance of the V coat between the cover and the waveguide material. For the optimization, RCWA was used to model a structure consisting of layers 4 and 5 on top of a substrate consisting of the waveguide material and the grating fill factor was adjusted to minimize the reflectance. Note in Fig. 6 that symmetry is preserved as the spectral width is adjusted even at narrow spectral widths. Figure 7 shows the relationship between the spectral width and the thickness of the waveguide layer.

In practice there is a lower bound on the spectral width that can be obtained with a GMR filter. Several authors[10,13,23] have suggested that scattering and other dissipative losses can limit the width of a resonant peak. The effect of these losses is to reduce the peak efficiency and broaden the width of the resonance. These effects are minimized when

$$\gamma_d \ll \gamma_c\,, \tag{5}$$

where γ_d represents the dissipative losses of the leaky mode and γ_c represents the coupling loss. As the dissipative loss approaches the coupling loss, the width of the resonance will be larger than expected and the peak efficiency will drop. A lower bound on spectral width can be estimated from the dissipative loss for a typical planar waveguide. If L is defined as the waveguide loss in units of decibels per centimeter, then

$$\gamma_d = L/[20\,\log_{10}(e)]\,. \tag{6}$$

Using a typical loss value of $L = 1$ dB/cm,[24] Eqs. (4) and (6) and inequality (5) can be used to calculate a lower bound on the spectral width as

$$\Delta\lambda_{\mathrm{FWHM}} \gg 0.0044 \text{ nm} \tag{7}$$

Table 1. Estimated Size of GMR Filters for Telecommunication Applications

Channel Spacing (GHz)	Channel Spacing (nm)	Spectral Width (nm)	Device Size (cm)
200	1.6	0.40	0.8
100	0.8	0.20	1.6
50	0.4	0.10	3.1

for a resonant wavelength of $\lambda_0 = 1550$ nm and a grating period of $\Lambda = \lambda_0/2$. In practice, one would expect the bound on the spectral width to be larger owing to grating fabrication errors, which have been neglected here.

Another factor that can limit the minimum spectral width is finite grating and beam size. The effect of finite size is to lower the efficiency and broaden the spectral width. Saarinen *et al.*,[25] estimated that the number of grating periods required to make the effects of finite grating size negligible is given by

$$N = C\lambda_0/\Delta\lambda_{\mathrm{FWHM}}\,, \tag{8}$$

where N is the number of grating periods and C is a proportionality constant of the order of unity. Therefore, the required width of grating area w can be written by use of Eq. (4) as

$$w \cong \Lambda\lambda_0/\Delta\lambda_{\mathrm{FWHM}} = \pi/\gamma\,, \tag{9}$$

when $C \cong 1$. This expression is in agreement with other approximate models[26–28] for the effect of finite grating size and experiments[27] for single leaky-mode filters. Avrutsky and Sychugov[23] investigated the effects of finite beam size and found that the beam diameter should satisfy the following relation:

$$a\gamma \gg 1\,, \tag{10}$$

where a is the beam diameter. From their results, peak efficiencies greater than 90% can be obtained when $a\,\gamma \approx 5$ for a Gaussian beam.

Consider a GMR filter with a spectral width equal to the lower bound given in Eq. (7). According to relation (9) and inequality (10), the grating area should be at least 27 cm wide and it should be used with beams of the order of 43 cm in diameter. Thus, the effects of finite grating area and beam size can be more significant than the effects of dissipative losses.

An important application for narrowband filters is in optical telecommunication systems. Table 1 shows the estimated device size for GMR filters for WDM applications. The device sizes are estimated as the sum of the finite grating and beam size criteria, assuming the resonance is associated with a single leaky mode, $\lambda_0 = 1550$ nm, and $\Lambda = \lambda_0/2$, i.e., size = $w + a$, where w is calculated from relation (9) and a is calculated from $a\,\gamma = 5$ by use of Eq. (4). In the 50-GHz case, the GMR filter should be larger than 1 in. (2.54 cm) in diameter, which might be a limiting factor when packaging issues are considered.

The finite beam size criterion can also be linked to

the angular tolerances for GMR filters. Norton *et al.*[12] showed that the angular width of a resonant peak is approximately given by

$$\Delta\theta = \lambda_0\gamma/(\pi\cos\theta)\,, \tag{11}$$

under the same assumptions that accompany Eq. (4), i.e., the resonance is associated with a single leaky mode. The angular divergence of a Gaussian beam[29] is given by

$$\delta\theta = 4\lambda/(\pi a)\,, \tag{12}$$

where a is the diameter of the beam waist. An obvious condition for high efficiency is that the beam divergence be much less than the angular width for the filter, i.e., $\delta\theta \ll \Delta\theta$. Using Eqs. (11) and (12), we can write this condition as

$$a \gg 4\cos\theta/\gamma\,, \tag{13}$$

which agrees with the condition given above for a in inequality (10). Thus, if the angular width of the resonance can be increased, smaller device sizes might be possible. Lemarchand *et al.*[30] and Jacob *et al.*[31] have reported on increasing the angular width of GMR filters operating at normal incidence. Such effects are based on interactions between forward-propagating and backpropagating leaky modes.

4. Passband Shaping

The spectral response of a GMR filter near resonance is characterized by Lorentzian-like behavior. This is a general characteristic of forced oscillating systems near resonance,[32] such as damped mechanical oscillators and RLC electric circuits. A Lorentzian line shape is characterized by a narrow rounded peak with rather slow sideband transitions. Many applications require a more rectangular spectral response, i.e., a flatter passband with sharper sideband transitions. Interference effects are often used for passband shaping in the design of traditional thin-film filters. A single-cavity Fabry–Perot filter is a classic thin-film design for a narrowband filter. However, the spectral response for a single-cavity filter has a narrow peak with slow sideband transitions, making it unsuitable for many applications. The transmitted and reflected fields from a Fabry–Perot filter undergo a 180-deg phase shift through the passband. This phase shift is exploited by stacking multiple Fabry–Perot filters on top of one another such that multiple reflections interfere constructively inside the passband and destructively outside the passband. The result is a more rectangular passband for the stacked filter.[1,2]

Similarly, interference effects can be used for passband shaping with GMR filters. Jacob *et al.*[15] showed that stacking identical GMR filters together, such that multiple reflections interfere constructively at the design wavelength, results in a more rectangular passband. However, strong sidelobes form when more than two filters are stacked together this way. We have found that the sidelobes can be eliminated, at least for the case of a four-filter stack, by adjustment of the spacing between filters. Specifically, the spacing between the second and the third filters is increased by a quarter wave. Figure 8 illustrates a stack of four identical GMR filters designed as a 200-GHz WDM filter. Figure 9 shows the spectral response for the stacked GMR filter of Fig. 8. For comparison, Fig. 9 also shows the spectral response of a conventional 200-GHz WDM thin-film filter taken from Ref. 2. Note that spectral responses are nearly equivalent. The performance specifications for the filters require that the spectral width be at least 0.7 nm at −0.3 dB and less than 2.5 nm at −20 dB.

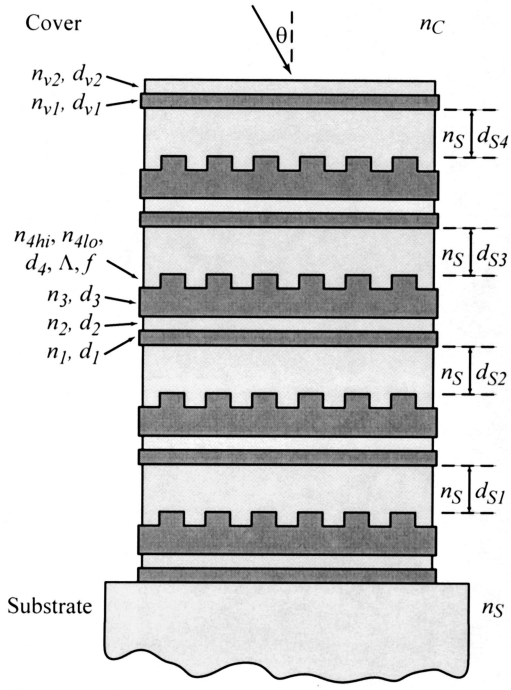

Fig. 8. Illustration of a stack of four GMR filters. Each filter is identical and made up of a V coat, a waveguide layer, and an antireflective grating layer. d_{s1}, d_{s2}, d_{s3}, and d_{s4} represent the thicknesses of the spacer layers between the filters. An additional V coat is on top of the stack. The design parameters are $n_s = n_2 = n_{4lo} = n_{v2} = 1.500$, $n_1 = n_3 = n_{4hi} = n_{v1} = 2.000$, $n_c = 1.000$, $d_1 = 64$ nm, $d_2 = 85$ nm, $d_3 = 1027$ nm, $d_4 = 238$ nm, $\Lambda = 769$ nm, $f = 30\%$, $d_{s1} = 1520$ nm, $d_{s2} = 1808$ nm, $d_{s3} = 1520$ nm, $d_{s4} = 600$ nm, $d_{v1} = 292$ nm, $d_{v2} = 195$ nm, and $\theta = 5$ deg.

We designed the GMR filter by first constructing a single symmetric GMR filter with the appropriate spectral width using the techniques described in the previous sections. Then, several of these filters were stacked together. The spacing between filters was determined in a manner analogous to that of Jacob *et al.*,[15] with the exception that the spacing between the middle pair of filters was increased by a quarter wave. This change eliminates the sidelobes, allowing the filter to meet the design specifications. Finally, a V coat was added to the top of the stack and the cover region was set to air. The spacers are thick enough such that

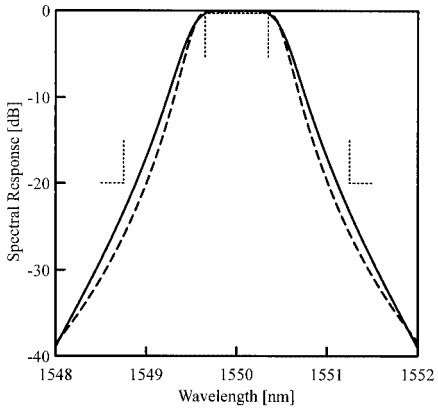

Fig. 9. Spectral response of two 200-GHz WDM filters. The solid curve represents the stacked GMR filter of Fig. 9, which operates in reflection, whereas the dashed curve represents a three-cavity Fabry–Perot thin-film filter, which operates in transmission. The design of the thin-film filter is taken from Ref. 2: A $|LH\ (HL)^7\ 6H\ (LH)^7\ L\ (HL)^7\ 6H\ (LH)^7\ L\ (HL)^7\ 6H\ (LH)^7|$ G, where $L = 303.51$ nm, $H = 94.4$ nm, each H and L represents a quarter-wave layer of the high- and low-index materials, and the indices of refraction are $n_A = 1.000$, $n_L = 1.444$, $n_H = 2.100$, and $n_G = 1.500$. The design wavelength is $\lambda_0 = 1550$ nm and the angle of incidence is $\theta = 0$ deg. The dotted lines indicate the filter specifications.

neighboring GMR filters do not perturb the leaky-mode propagation coefficients.

5. Fabrication Tolerances

It is important to consider fabrication tolerances for narrowband filters. Often, thin-film WDM filters have extremely tight tolerances. Macleod's tolerance analysis for the 90-layer thin-film filter of Fig. 9 yielded random thickness tolerances of 0.003% without compensation.[2] This corresponds to absolute tolerances of 0.006 and 0.008 nm on the quarter-wave H and L layers, respectively, which are impossible to meet. However, since most of the layers are quarter wave, optical monitoring can be used during fabrication to compensate for thickness errors in lower layers.

We present a tolerance analysis of the stacked GMR filter for comparison. Table 2 shows the tolerances for each design parameter, whereas Fig. 10 shows the effect of fabrication errors on the spectral response. Although the nominal values for each GMR filter in the stack are identical, all the errors were applied to each layer independently, with the exception of the grating period. The period was the same for each grating layer because of limitations in our implementation of RCWA. Note that the thickness tolerances for the GMR filter are much looser than those for the thin-film filter. It is interesting to note that the primary effect of fabrication errors on the thin-film filter was to degrade the passband, whereas the primary effect on the GMR filter was to degrade the sidebands.

Even though the thickness tolerances for the GMR filter can be relatively loose, the presence of embedded grating layers complicates fabrication. Furthermore, the tolerances for the grating period and profile are tight. One possible method for fabricating the embedded gratings is ion implantation.[33] Ion implantation would produce gratings with smaller index modulations that are likely to have looser tolerances on the grating profile. Errors in the fill factor change the effective index of the grating layer, but, if the grating modulation is small, the effective-index will be less sensitive to these errors. The individual GMR filters in the stack would need to be redesigned to achieve the same passband width with a smaller modulation. It is interesting to note from Table 2 that offsets between gratings are essentially irrelevant. An intuitive explanation of this is that all the gratings are subwavelength and effectively act as homogeneous thin films.

Another important consideration is the required diffraction efficiency for each of the GMR filters. If the insertion loss specification is 0.3 dB and there are four GMR filters in the stack, then each filter should have a peak efficiency greater than 98%. In 1990, Gale *et al.*[34] demonstrated a peak efficiency of the

Table 2. Tolerance Analysis of GMR 200-GHz Telecommunication Filter

Parameter	Nominal Value	Relative Tolerance (%)	Absolute Tolerance
d_{v1}	195.1 nm	1	2.0 nm
d_{v2}	291.8 nm	1	2.9 nm
d_{s4}	600.4 nm	1	6.0 nm
d_{s3}	1549.6 nm	0.1	1.5 nm
d_{s2}	1808.4 nm	0.2	3.6 nm
d_{s1}	1549.6 nm	0.1	1.5 nm
d_4	238.1 nm	0.5	1.2 nm
d_3	1027.0 nm	0.02	0.2 nm
d_2	85.3 nm	0.5	0.4 nm
d_1	63.9 nm	0.5	0.3 nm
Λ	768.661 nm	0.001	0.008 nm
f	30.01%	0.5	0.15%
a	230.7 nm	0.5	1.2 nm
Grating offset	0 nm	—	769 nm

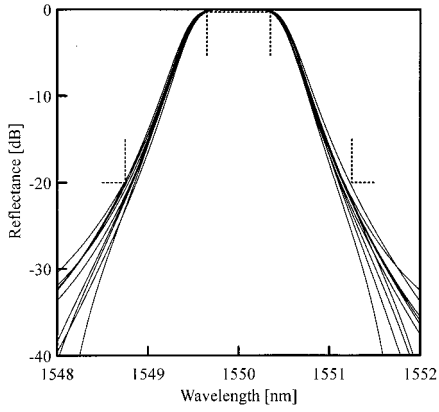

Fig. 10. Spectral response for an ensemble of GMR filters based on the design of Fig. 8 with random fabrication errors. Table 2 shows the nominal value and standard deviation for each design parameter. The dotted lines indicate the filter specifications.

order of 90% for a one-dimensional embedded GMR structure operating with TM-polarized light. They fabricated a surface-relief grating by embossing and then evaporated material on top of the grating. More recently Liu *et al.*[35] obtained a peak efficiency of 98% for a one-dimensional structure operating with TE-polarized light. Peng and Morris[36] fabricated a polarization-independent two-dimensional GMR filter with a peak efficiency of 62%.

6. Conclusion

Guided-mode resonance filters have been suggested for use in a large number of applications, but so far their use has been impractical in most cases. Many applications place requirements on the spectral response for a filter that designers have not been able to meet. As design methods for GMR filters improve, their use in practical situations becomes more likely. Here we have shown that techniques for controlling the spectral width can be used in conjunction with the thin-film design method, which provides control over symmetry and sideband levels. Furthermore, one can take advantage of interference effects for passband shaping.

Several other issues can limit the use of GMR filters in practice. Dissipative losses, finite grating, and finite beam size broaden the spectral width and reduce the peak efficiency for a filter. Dissipative loss values of the order of a few decibels per centimeter, which is typical for a planar waveguide, are negligible for most applications. However, the loss is likely to be much higher in GMR filters because of grating fabrication errors. As the spectral width decreases the device size required for acceptable performance increases and could eventually become prohibitive. For example, the required size for a 50-GHz WDM filter was estimated to be of the order of 3 cm, which might conflict with telecom packaging constraints. Smaller device sizes might be possible for filters that exhibit interactions between forward propagating and backpropagating leaky modes.

GMR filters have some advantages and disadvantages when compared with conventional thin-film filters. As an example, we compared GMR and thin-film designs of a 200-GHz WDM filter. The GMR design has fewer layers, but at the cost of fabricating four embedded grating layers. Fewer layers lead to looser thickness tolerances, but tolerances for the grating period and profile are tight. The alignment of each grating relative to the others is irrelevant.

The authors thank Daniel H. Raguin and Tasso R. M. Sales for their helpful discussions, insights, and suggestions, as well as their assistance with tolerancing the stacked GMR filter. This research was supported by Corning, Incorporated.

References

1. H. A. Macleod, *Thin-Film Optical Filters* (American Elsevier, New York, 1969).
2. H. A. Macleod, "Challenges in the design and production of narrow-band filters for optical fiber telecommunications," in *Optical and Infrared Thin Films*, M. L. Fulton, ed., Proc. SPIE **4094,** 46–57 (2000).
3. R. Magnusson and S. S. Wang, "New principle for optical filters," Appl. Phys. Lett. **61,** 1022–1024 (1992).
4. J. A. Cox, R. A. Morgan, R. Wilke, and C. M. Ford, "Guided-mode grating resonant filters for VCSEL applications," in *Diffractive and Holographic Device Technologies and Applications V*, I. Cindrich and S. H. Lee, eds., Proc. SPIE **3291,** 70–76 (1998).
5. A. Sharon, D. Rosenblatt, A. A. Friesem, H. G. Weber, H. Engel, and R. Steingrueber, "Light modulation with resonant grating-waveguide structures," Opt. Lett. **21,** 1564–1566 (1996).
6. S. M. Norton, "Resonant grating structures: theory, design, and applications," Ph.D. dissertation (University of Rochester, Rochester, N.Y., 1997).
7. G. A. Golubenko, V. A. Sychugov, and A. V. Tishchenko, "The phenomenon of full 'external' reflection of light from the surface of a corrugated dielectric waveguide and its use in narrow band filters," Sov. Phys. Lebedev Inst. Rep. **1**(11), 36–40 (1985).
8. S. S. Wang and R. Magnusson, "Design of waveguide-grating filters with symmetrical line shapes and low sidebands," Opt. Lett. **19,** 919–921 (1994).
9. Z. Hegedus and R. Netterfield, "Low sideband guided-mode resonant filter," Appl. Opt. **39,** 1469–1473 (2000).
10. U. Fano, "The theory of anomalous diffraction gratings and of quasi-stationary waves on metallic surfaces (Sommerfeld's waves)," J. Opt. Soc. Am. **31,** 213–222 (1941).
11. A. Sharon, D. Rosenblatt, and A. A. Friesem, "Narrow spectral bandwidths with grating waveguide structures," Appl. Phys. Lett. **69,** 4154–4156 (1996).
12. S. M. Norton, T. Erdogan, and G. M. Morris, "Coupled-mode theory of resonant-grating filters," J. Opt. Soc. Am. A **14,** 629–639 (1997).
13. S. M. Norton, G. M. Morris, and T. Erdogan, "Experimental investigation of resonant-grating filter lineshapes in comparison with theoretical models," J. Opt. Soc. Am. A **15,** 464–472 (1998).
14. G. Levy-Yurista and A. A. Friesem, "Very narrow spectral filters with multilayered grating/waveguide structures," Appl. Phys. Lett. **77,** 1596–1598 (2000).
15. D. K. Jacob, S. C. Dunn, and M. G. Moharam, "Flat-top narrow-band spectral response obtained from cascaded resonant grating reflection filters," Appl. Opt. **41,** 1241–1245 (2002).
16. S. Tibuleac and R. Magnusson, "Narrow-linewidth bandpass filters with diffractive thin-film layers," Opt. Lett. **26,** 584–586 (2001).
17. S. T. Thurman and G. M. Morris, "Resonant-grating filter design: the appropriate effective-index model," presented at the OSA Annual Meeting, Providence, R.I., 22–26 Oct. 2000.
18. M. G. Moharam and T. K. Gaylord, "Rigorous coupled-wave analysis of planar-grating diffraction," J. Opt. Soc. Am. **71,** 811–818 (1981).
19. S. Peng and G. M. Morris, "An efficient implementation of rigorous coupled-wave analysis for surface-relief gratings," J. Opt. Soc. Am. A **12,** 1087–1096 (1995).
20. T. Tamir and S. T. Peng, "Analysis and design of grating couplers," Appl. Phys. **14,** 235–254 (1977).
21. S. M. Rytov, "Electromagnetic properties of a finely stratified medium," Sov. Phys. JETP **2,** 466–475 (1956).
22. M. Nevière, R. Petit, and M. Cadilhac, "About the theory of optical grating coupler/waveguide systems," Opt. Commun. **8,** 113–117 (1973).
23. I. A. Avrutsky and V. A. Sychugov, "Reflection of a beam of finite size from a corrugated waveguide," J. Mod. Opt. **36,** 1527–1539 (1989).

24. H. Nishihara, M. Haruna, and T. Suhara, "Materials and fabrication techniques," in *Optical Integrated Circuits* (McGraw-Hill, New York, 1989), pp. 138–171.
25. J. Saarinen, E. Noponen, and J. Turunen, "Guided-mode resonance filters of finite aperture," Opt. Eng. **34,** 2560–2566 (1995).
26. J. C. Brazas and L. Li, "Analysis of input-grating couplers having finite lengths," Appl. Opt. **34,** 3786–3792 (1995).
27. R. R. Boye and R. K. Kostuk, "Investigation of the effect of finite grating size on the performance of guided-mode resonance filters," Appl. Opt. **39,** 3649–3653 (2000).
28. D. K. Jacob, S. C. Cunn, and M. G. Moharam, "Design considerations for narrow-band dielectric resonant grating reflection filters of finite length," J. Opt. Soc. Am. A **17,** 1241–1249 (2000).
29. B. E. A. Saleh and M. C. Teich, *Fundamentals of Photonics* (Wiley-/Interscience, New York, 1991), pp. 80–107.
30. F. Lemarchand, A. Sentenac, and H. Giovannini, "Increasing the angular tolerance of resonant grating filters with doubly periodic structures," Opt. Lett. **23,** 1149–1151 (1998).
31. D. K. Jacob, S. C. Dunn, and M. G. Moharam, "Resonant grating reflection filters for normally incident Gaussian beams," in *Diffractive Optics and Micro-Optics*, Postconference Digest, Vol. 41 of OSA Trends in Optics and Photonics (Optical Society of America, Washington, D.C., 2000), pp. 23–25.
32. I. G. Main, "Forced vibrations," in *Vibrations and Waves in Physics* (Cambridge University Cambridge, England 1993), pp. 56–77.
33. P. D. Townsend, "An overview of ion-implanted optical waveguide profiles," Nucl. Instrum. Methods Phys. Res. B **46,** 18–25 (1990).
34. M. T. Gale, K. Knop, and R. H. Morf, "Zero-order diffractive microstructures for security applications," in *Optical Security and Anticounterfeiting Systems*, W. F. Fagan, ed., Proc. SPIE **1210,** 83–89 (1990).
35. Z. S. Liu, S. Tibuleac, D. Shin, P. P. Young, and R. Magnusson, "High-efficiency guided-/mode resonance filter," Opt. Lett. **23,** 1556–1558 (1998).
36. S. Peng and G. M. Morris, "Experimental demonstration of resonant anomalies in diffraction from two-dimensional gratings," Opt. Lett. **21,** 549–551 (1996).